JOINT INSTITUTE FOR NUCLEAR RESEARCH
Laboratory of Nuclear Problems

FINAL REPORT ON THE INTEREST PROGRAMME

"Monte Carlo simulation of radiation-matter interaction for shielding evaluation in medical imaging applications"

Student:
Alejandro Miguel Neyra Suárez
InSTEC, Habana, Cuba

Supervisor:
Dr. Antonio Leyva Fabelo

Consultant:
Lic. Elizabeth Vega Moreno

Participation period:
November 05 - December 14
Wave 11

Dubna, 2024

Abstract

The safety of individuals exposed to ionizing radiation in medical settings is crucial, especially with the use of advanced technologies such as the SPECT-CT scanner. This study focuses on mathematical simulations to analyze the dose rate distribution in a SPECT-CT system that utilizes a molybdenum X-ray tube for the CT and the radioisotopes ^{99m}Tc and ^{111}In for the SPECT. The Monte Carlo N-Particle (MCNPX) code was employed to conduct the simulations. The results indicate that the safe distances to avoid exceeding the dose limit of 2.3 μSv/h are found within the gantry, ensuring that this equipment does not require external shielding. This not only optimizes the safety of personnel and patients but also simplifies space design and reduces operational costs.

Introduction

The safety of personnel and visitors in environments that utilize ionizing radiation, such as in diagnostic and medical treatment techniques (X-rays, SPECT, CT), is crucial. Mathematical modeling of radiation transport allows for precise simulations of dose distribution, helping to establish safe and efficient conditions for the use of these systems. This study analyzes the dose rate distribution in configurations near preclinical SPECT-CT scanner aiming to estimate the minimum safe distance for health and to determine the optimal thickness of the lead protective wall.

Since Wilhelm Roentgen's discovery of X-rays, methods such as computed tomography and SPECT have been developed which, while improving diagnostic efficacy, also lead to increased radiation exposure. Therefore, it is essential to protect personnel and adjust doses for patients.

The primary objective of this work is to determine the safe working distance for occupationally exposed personnel, using the MCNPX code system based on the Monte Carlo method. The sub-objectives include familiarizing oneself with imaging techniques, studying mathematical modeling of radiation-matter interaction, and defining safe dose limits according to the literature.

Materials and Methods.

SPECT-CT tomography.

CT

Computed tomography (CT) (Figure 1.a) generates detailed cross-sectional images (Figure 1.b) by leveraging the differential attenuation of X-rays as they pass through the body. A rotating X-ray tube and detector array acquire multiple projection profiles from various angles. Modern scanners typically employ helical scanning, where continuous rotation and patient movement optimize data acquisition. Sophisticated algorithms, often based on iterative reconstruction or filtered back-projection, process these projections to reconstruct the spatial distribution of linear attenuation coefficients. This results in a series of high-resolution cross-sectional images representing tissue density variations. Multiple slices are integrated to create three-dimensional datasets, allowing for advanced visualization techniques crucial for diagnosis and surgical planning [1].

a

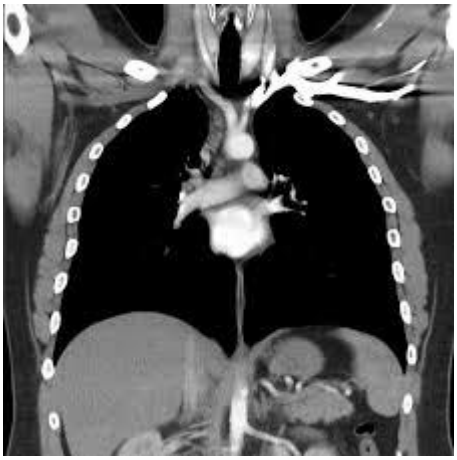

b

Figure 1. a) CT scanner b) Image taken with the CT technique

Although it is a very useful technique, it is advisable to expose the patient to it only, if necessary, due to the exposure to ionizing radiation, which could have medical consequences in the future.

SPECT

Single-photon emission computed tomography (SPECT) (Figure 2.a) is a nuclear medicine imaging technique visualizing the distribution of radiopharmaceuticals within the body to assess organ function. A gamma-emitting radiopharmaceutical, targeted to a specific organ or process, is administered. The emitted gamma rays are detected by a rotating gamma camera equipped with a collimator to precisely locate the emissions.

Sophisticated algorithms reconstruct the acquired data into three-dimensional images reflecting the radiotracer concentration, providing functional information about the targeted area. While offering valuable insights into physiological processes, SPECT has limitations including lower resolution than other modalities and radiation exposure. The technique's strength lies in its ability to visualize functional processes (Figure 2.b), making it a valuable tool in various medical fields [2].

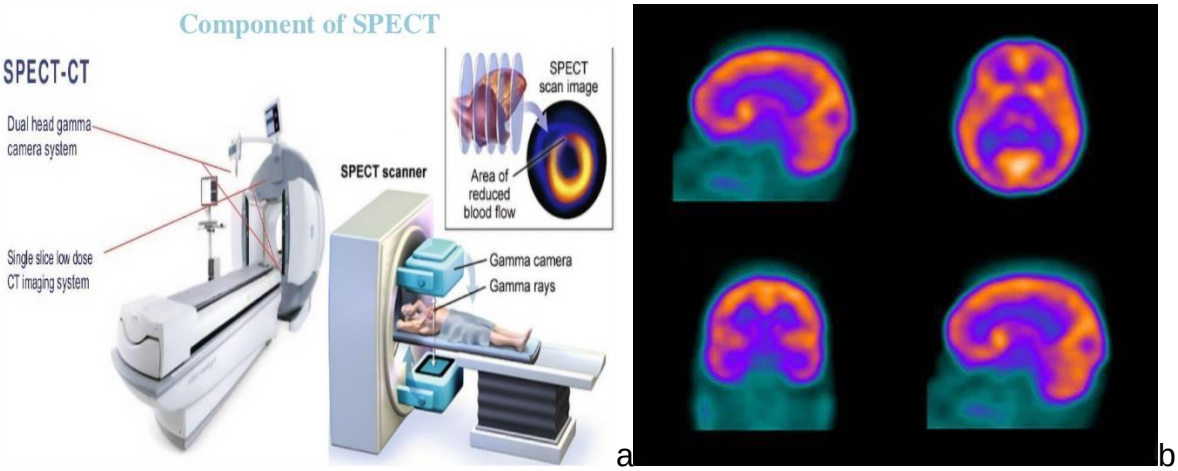

a b

Figure 2. a) Components of SPECT. b) Image taken with the SPECT technique

SPECT-CT

SPECT-CT (Figure 3.a) represents a significant advancement in nuclear medicine, synergistically combining the functional capabilities of single-photon emission computed tomography (SPECT) with the high-resolution anatomical detail provided by computed tomography (CT). This integration overcomes limitations inherent in each modality when used independently, resulting in enhanced diagnostic accuracy and improved clinical workflow.

The system integrates a gamma camera and a CT scanner within a single gantry. Following the administration of a targeted radiopharmaceutical, the gamma camera acquires projection data of gamma ray emissions resulting from radionuclide decay. Concurrently, the CT scanner obtains high-resolution anatomical images. Sophisticated image reconstruction algorithms, applied separately to each dataset, generate a functional SPECT image reflecting radiotracer distribution and a detailed anatomical CT image. A crucial step involves image registration, precisely aligning the SPECT and CT

datasets using algorithms that identify corresponding anatomical landmarks. This co-registration allows for the fusion of the functional and anatomical information, resulting in images where the SPECT data overlays the precisely defined anatomical structures from the CT scan [3].

This integration offers substantial advantages (Figure 3.b). Firstly, the precise anatomical localization from CT overcomes the limitations of SPECT's spatial resolution, resolving ambiguity in the location of functional abnormalities within complex anatomical regions. Secondly, CT data facilitates accurate attenuation correction for SPECT, improving the quantitative analysis of radiotracer distribution by compensating for the reduction in gamma ray intensity as it traverses different tissue densities. Thirdly, the combined information significantly increases diagnostic accuracy, enhancing the sensitivity and specificity of the interpretation of functional abnormalities. Finally, the simultaneous acquisition of both datasets improves patient workflow and minimizes radiation exposure compared to sequential imaging procedures [4].


a
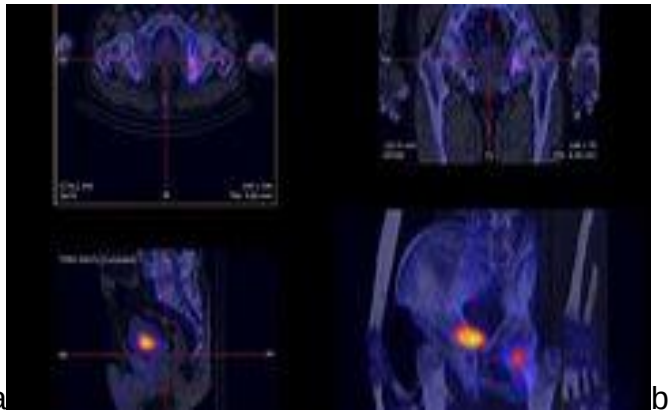
b

Figure 3. a) SPECT-CT scanner b) Image taken with a SPECT-CT system.

SPECT-CT provides a superior imaging modality by integrating functional and anatomical information, leading to improved diagnostic capabilities, and facilitating more informed treatment planning across a wide spectrum of clinical applications. The synergistic combination of SPECT-CT represents a substantial enhancement in medical imaging technology.

Sources used in SPECT-CT.

The acquisition of high-quality images in Single-Photon Emission Computed Tomography (SPECT) is critically dependent on the selection of the appropriate radiopharmaceutical. While a broad range of radionuclides are available, certain isotopes have established

themselves as the most widely used due to their favorable characteristics in terms of emission properties, half-life, and availability.

^{99m}Tc reigns as the most prevalent radionuclide employed in SPECT-CT. This dominance stems from a confluence of advantageous factors. It emits gamma rays of 140 keV, an energy ideal for SPECT image acquisition, providing good detection efficiency with minimal tissue attenuation. Its 6-hour half-life facilitates the imaging of multiple organs without excessive patient radiation exposure, contributing to a favorable benefit-risk ratio. Its production via ^{99}Mo/^{99m}Tc generators renders it readily accessible and relatively inexpensive, significantly contributing to its widespread use. The diverse chemistry of ^{99m}Tc allows its incorporation into a vast array of radiopharmaceuticals targeted at various organs and systems, greatly expanding its clinical utility [5].

While not as ubiquitous as ^{99m}Tc, ^{111}In plays a significant role in SPECT-CT, particularly in applications demanding specific characteristics. ^{111}In emits gamma rays at 171 keV and 245 keV. This feature enables attenuation and scatter correction during image acquisition, enhancing image quality, although image processing is more computationally intensive. Its 2.8-day half-life permits the monitoring of biological processes over an extended period. This is particularly valuable in studies requiring long-term tracking. ^{111}In is frequently utilized in radiopharmaceuticals targeting specific receptors, enabling the visualization of immunological processes and tumor localization through labeled antibodies. This isotope finds use in labeled leukocyte studies for infection detection and lymphocyte studies for metastasis and tumor detection [6].

In our simulation, ^{99m}Tc and ^{111}In will be used as radionuclides to label the radiopharmaceutical for SPECT imaging.

Other radionuclides, such as ^{123}I (Iodine-123) and ^{67}Ga (Gallium-67), also find niche applications in SPECT-CT, although their use is more specialized due to considerations such as half-life, emission energy, and availability.

In X-rays mammography, molybdenum (Mo) anodes offer significant advantages over the tungsten (W) anodes typically used in general-purpose computed tomography (CT). Molybdenum's characteristic X-rays, primarily at 17 keV and 19 keV, possess lower energy than those emitted by tungsten. This lower-energy spectrum is crucial for breast

imaging because it enhances contrast between different breast tissue densities (fat, glandular, and fibroglandular tissue) while simultaneously reducing patient radiation dose. The lower energy photons are more effectively absorbed by soft tissues, improving the visualization of subtle differences critical for differentiating benign from malignant lesions. Careful filtration techniques, often incorporating molybdenum filters, are employed to further refine the spectrum, maximizing the contrast-enhancing portion while minimizing the higher-energy components that contribute disproportionately to dose [7].

The lower-energy spectrum of molybdenum, however, limits its penetration. This restricts its use primarily to mammography of breasts with lower density or smaller size. For denser or larger breasts, alternative techniques or higher-energy X-ray sources might be required to achieve adequate image penetration. The trade-off, therefore, lies in optimizing image quality and patient radiation exposure: for cases where molybdenum's spectral characteristics are advantageous, the reduction in dose and enhancement in contrast significantly outweigh the limitations imposed by its reduced penetration.

In our simulations a Molybdenum Roentgen tube is used as source of X-rays. For simplicity in calculus, the anode in the X-ray tube was approximated to a point-like source positioned 1 mm in front of a hypothetical tungsten anode. Within a solid angle of 20^{o}, this source emits only in the target direction.

Dose safe limits.

Radiation protection relies on the application of optimization and dose limitation principles to minimize adverse effects from ionizing radiation exposure. These principles are embodied in the establishment of safe dose limits, differentiated for occupationally exposed workers and the general public. These limits, set by the International Commission on Radiological Protection (ICRP), are based on the assessment of both deterministic and stochastic risks associated with radiation exposure. Deterministic effects, which occur with certainty above a threshold dose, are prevented by setting dose limits below that threshold. Stochastic effects, such as cancer, lack a defined threshold, and their probability of occurrence increases with dose; therefore, the strategy is to limit dose to minimize the probability of their occurrence.

For occupationally exposed workers, the ICRP recommends annual dose limits of 20 mSv effective dose, 20 mSv equivalent dose to the lens of the eye, and 500 mSv equivalent

dose to the skin (averaged over 1 cm^2) and extremities. These limits reflect the higher radiation tolerance in individuals with continuous exposure through the control and monitoring of their dose [8].

In contrast, the general public, not involved in activities with ionizing radiation, has considerably lower dose limits: 1 mSv effective dose annually, 15 mSv equivalent dose to the lens of the eye, and 50 mSv equivalent dose to the skin (averaged over 1 cm^2). These stricter values protect the public from exposure to external radiation sources, reflecting their greater vulnerability to harmful effects.

It's crucial to note that these limits exclude medical exposure and natural background radiation. Annual effective dose in medical procedures is considered safe within an approximate range of 1-20 mSv per year, although this varies depending on the type of radiological study and the patient's age. Procedures such as a chest X-ray typically involve a dose of 0.1-0.2 mSv, while an abdominal CT scan may be around 10 mSv. In interventional procedures like fluoroscopy, dose limitation is rigorously controlled to ensure the safety of both patients and medical staff [8].

Interaction of photons with matter [9].

Photons (X-ray and gamma) end their lives by transferring their energy to electrons contained in matter. X-rays are important in diagnostic examinations for many reasons. For example, the selective interaction of X-ray photons with the structure of the human body produces the image, the interaction of photons with the receptor converts an X-ray or gamma image into one that can be viewed or recorded.

Photons are individual units of energy. As an X-ray beam or gamma radiation passes through an object, three possible fates await each photon.

1. It can penetrate the section of matter without interacting.
2. It can interact with the matter and be completely absorbed by depositing its energy.
3. It can interact and be scattered or deflected from its original direction and deposit part of its energy.

The main mechanisms of interactions of photons with matter are:

Photoelectric

In the photoelectric (photon-electron) interaction, as shown above, a photon transfers all its energy to an electron located in one of the atomic shells. The electron is ejected from the atom by this energy and begins to pass through the surrounding matter. The electron rapidly loses its energy and moves only a relatively short distance from its original location. The photon's energy is, therefore, deposited in the matter close to the site of the photoelectric interaction.

The energy transfer is a two-step process. The photoelectric interaction in which the photon transfers its energy to the electron is the first step. The depositing of the energy in the surrounding matter by the electron is the second step. Photoelectric interactions usually occur with electrons that are firmly bound to the atom, that is, those with a relatively high binding energy.

Photoelectric interactions are most probable when the electron binding energy is only slightly less than the energy of the photon. If the binding energy is more than the energy of the photon, a photoelectric interaction cannot occur. This interaction is possible only when the photon has sufficient energy to overcome the binding energy and remove the electron from the atom. The photon's energy is divided into two parts by the interaction. A portion of the energy is used to overcome the electron's binding energy and to remove it from the atom. The remaining energy is transferred to the electron as kinetic energy and is deposited near the interaction site. Since the interaction creates a vacancy in one of the electron shells, typically the K or L, an electron moves down to fill in. The drop in energy of the filling electron often produces a characteristic X-ray photon. The energy of the characteristic radiation depends on the binding energy of the electrons involved.

Compton

A Compton interaction is one in which only a portion of the energy is absorbed and a photon is produced with reduced energy. This photon leaves the site of the interaction in a direction different from that of the original photon, as shown in the previous figure. Because of the change in photon direction, this type of interaction is classified as a scattering process. In effect, a portion of the incident radiation "bounces off' or is scattered by the material. This is significant in some situations, because the material within the

primary X-ray beam becomes a secondary radiation source. The most significant object producing scattered radiation in an X-ray procedure is the patient's body. The portion of the patient's body that is within the primary X-ray beam becomes the actual source of scattered radiation. This has two undesirable consequences. The scattered radiation that continues in the forward, direction and reaches the image receptor decreases the quality (contrast) of the image; the radiation that is scattered from the patient is the predominant source of radiation exposure to the personnel conducting the examination.

Coherent scatter

There are actually two types of interactions that produce scattered radiation. One type, referred to by a variety of names, including coherent, Thompson, Rayleigh, classical, and elastic, is a pure scattering interaction and deposits no energy in the material. Although this type of interaction is possible at low photon energies, it is generally not significant in most diagnostic procedures.

Pair production

Pair production is a photon-matter interaction that is not encountered in diagnostic procedures because it can occur only with photons with energies in excess of 1.02 MeV. In a pair-production interaction, the photon interacts with the nucleus in such a manner that its energy is converted into matter. The interaction produces a pair of particles, an electron and a positively charged positron. These two particles have the same mass, each equivalent to a rest mass energy of 0.51 MeV.

Monte Carlo method.

Monte Carlo methods comprise a broad class of computational statistical techniques employing repeated random sampling to generate simulations and derive numerical solutions for complex problems. These methods are particularly advantageous for problems lacking analytical solutions or those where obtaining analytical or numerical solutions is computationally prohibitive. The continuous advancements in computational power have significantly expanded the applicability of Monte Carlo methods across diverse scientific disciplines.

The fundamental approach of Monte Carlo simulation involves three key steps: 1) the development of a model accurately representing the system under investigation, including the precise definition of its input variables; 2) the generation of random inputs within the model framework, based on established probability density functions (PDFs), with subsequent recording of the corresponding output variables; and 3) iterative repetition of step 2 to ensure convergence according to the Law of Large Numbers (LLN), culminating in the aggregation of results to yield a statistically robust estimate. Probability density functions (PDFs) quantify the relative likelihood of a continuous random variable assuming a given value, providing the essential a priori information for the sampling process. As the number of simulated events (histories) increases, the accuracy of the average behavior of the system's output variables improves, in accordance with the LLN, thereby reducing the associated statistical uncertainty [10].

MCNPX for modeling radiation transport in matter.

MCNPX (Monte Carlo N-Particle eXtended) is a versatile, general-purpose Monte Carlo radiation transport code capable of simulating the interactions of 34 particle types (including nucleons, ions, and over 2000 heavy ions) across a wide energy range. The code models complex three-dimensional geometries using first- and second-degree surfaces, as well as fourth-degree elliptical tori, allowing for the accurate representation of arbitrary material configurations. For photons, MCNPX accounts for incoherent and coherent scattering, fluorescence following photoelectric absorption, pair production with annihilation radiation, and bremsstrahlung. Electron transport, including positrons, K X-rays, and bremsstrahlung, utilizes a continuous-slowing-down approximation, although external or self-induced fields are not considered [11].

The code's extensive capabilities include a flexible tally structure, a variety of variance reduction techniques, and an extensive cross-section data library. Its powerful source definition options (general, criticality, and surface sources), along with integrated geometry and output plotters, enhance usability and facilitate data analysis. MCNPX's primary value lies in its predictive capabilities, offering a cost-effective and often indispensable alternative to expensive or infeasible experimental approaches.

In the medical physics domain, MCNPX plays a critical role in radiation therapy treatment planning, simulating dose distributions in tissues and organs. This includes calculating the dose delivered to the tumor and surrounding healthy tissue, crucial for optimizing

treatment plans and minimizing side effects. The code accurately simulates photon and electron beams employed in radiation therapy and is extensively used for the design and evaluation of shielding in medical facilities, such as radiation therapy rooms and nuclear medicine laboratories. Furthermore, MCNPX enables verification of dosimeter readings against in vivo measurements and supports research into novel treatment modalities, such as proton and heavy ion therapy. Its applications extend to evaluating radiation doses received during imaging procedures (CT scans, gammagraphy), contributing to the development of safer and more efficient imaging protocols. Through its detailed modeling of particle interactions and sophisticated simulation capabilities, MCNPX provides a powerful tool for advancing medical physics research and improving patient care.

Results.

SPECT

In Figure 4, the dose rate as a function of distance for ^{99m}Tc is presented. It is observed that the distance at which the dose rate remains below the permissible limit is 22.62 cm from the source. This point is located within the gantry, before reaching the distance where a lead wall would be placed, approximately 32 cm away.

This finding indicates that, since the dose rate does not exceed safe levels within this distance, there is no need to install a lead wall for this equipment. Implementing a lead barrier could incur additional costs and complicate the design of the space. Therefore, by keeping the dose rate within acceptable limits, safety can be optimized without the need for extra protective measures.

In Figure 5, the dose rate as a function of distance for ^{111}In is shown. It is observed that the distance at which the permissible dose limit is not exceeded is 27.63 cm from the source. Similar to technetium-99m, this point is also located within the gantry, indicating that a lead wall is not necessary in this case either.

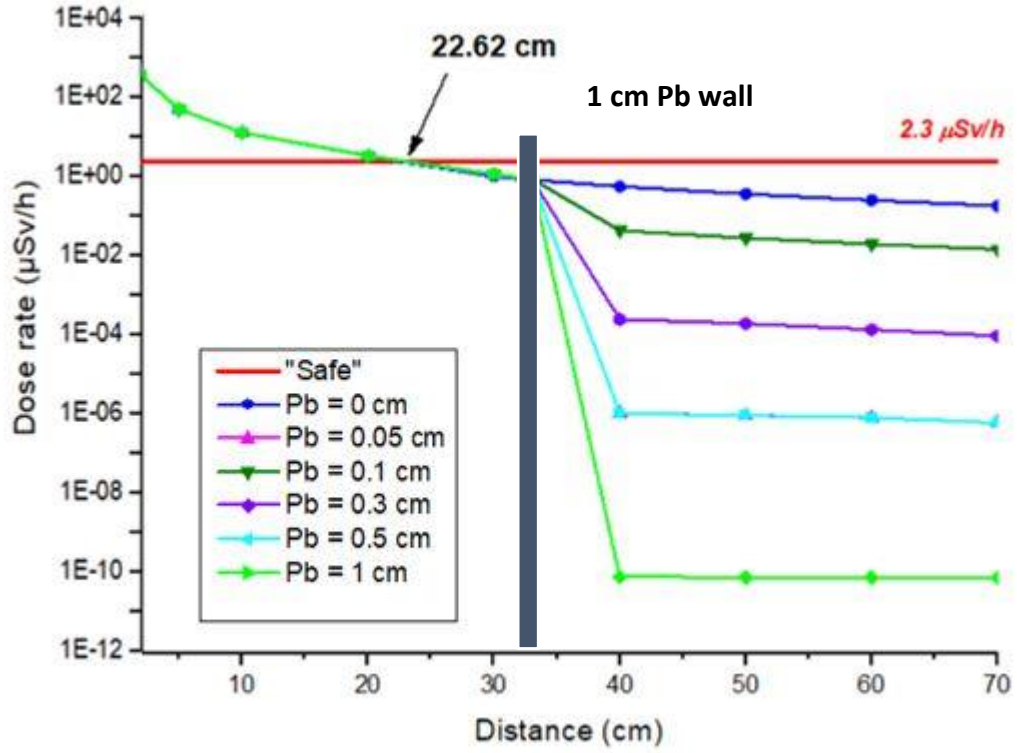

Figure 4. Dose rate as a function of distance for ^{99m}Tc.

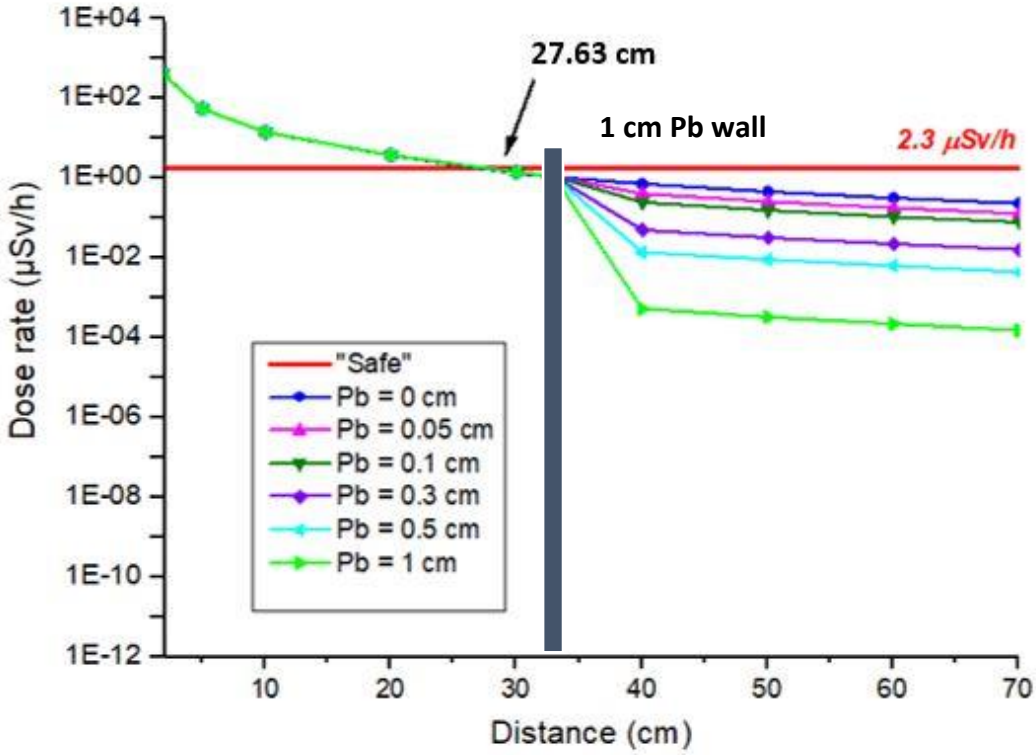

Figure 5. Dose rate as a function of distance for ^{111}In.

The analysis of dose rates for both ^{99m}Tc and ^{111}In indicates that external shielding is not required for this equipment. These findings suggest that since the dose rates are maintained within safe levels, there is no need to install lead shielding. This avoids additional costs and design complications while ensuring optimal safety.

CT

In Figure 6, the graph of the dose rate as a function of distance for the computed tomography (CT) using a Mo X-ray tube source is shown. It can be observed that, for the energies of the molybdenum X-ray tube, external shielding is not necessary. This is because the minimum safe distance to avoid reaching the dose limit is within the gantry.

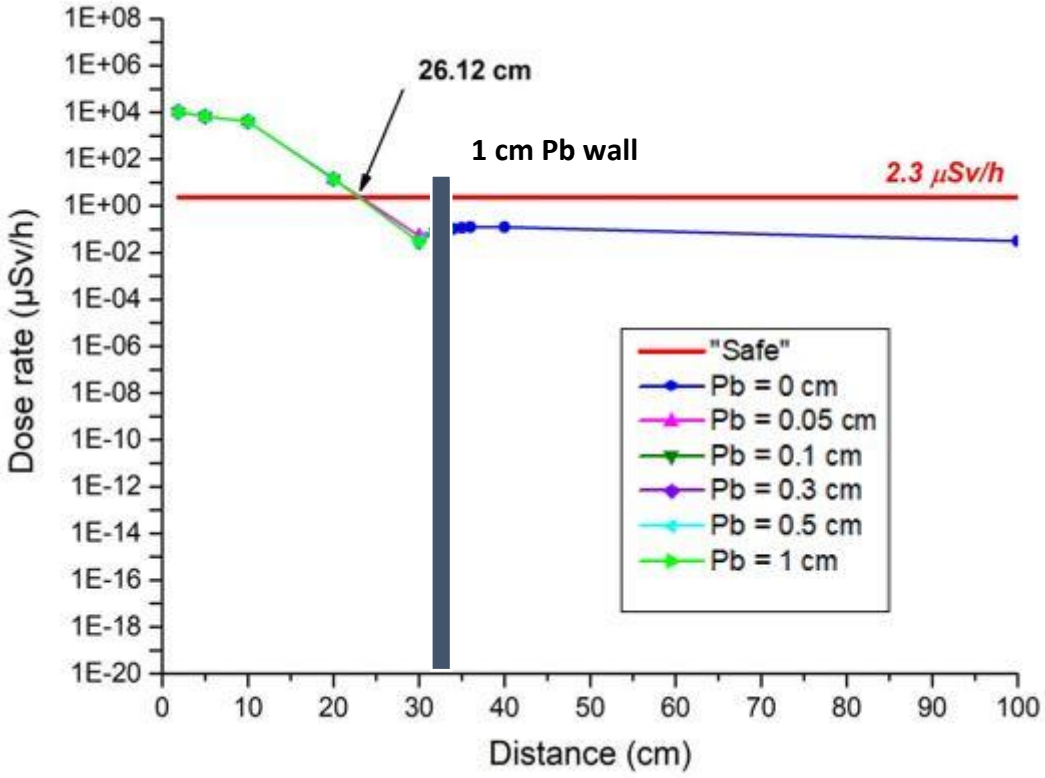

Figure 6. Dose rate as a function of distance for CT.

Since the dose rate remains below permissible levels in this area, it can be concluded that implementing additional shielding would be unnecessary. The gantry design is sufficient to provide effective protection without the need for external shielding materials.

Conclusions.

1- By utilizing the Monte Carlo N-Particle (MCNPX) code system, which operates on the Monte Carlo method, we were able to simulate the distribution of dose rates in a preclinical SPECT-CT imaging scanner. For this detailed analysis, a molybdenum X-ray tube was used for the CT component, along with two different gamma radionuclides for the SPECT component. Additionally, we varied the thickness of a lead wall between 0 cm and 2 cm. The dose rates for each geometric configuration were measured at various distances from the source in both scenarios and compared to the internationally recognized safe dose limit of 2.3 μSv/h

2- The simulation reveals that, in the case of the computed tomography (CT) scanner with a molybdenum tube, external shielding is not required. This is because safe distances to avoid exposure to harmful doses are achieved from within the gantry. Since the gantry acts as a physical barrier protecting both personnel and patients, the equipment configuration ensures that the radiation source does not pose a significant risk.

3- The data obtained for ^{99m}Tc and ^{111}In as sources for the SPECT scanner indicate that safe distances are also achieved within the gantry in both cases. This is crucial, as it means that the equipment design already provides effective protection against radiation. By keeping dose rates below established limits, the risk of exposure for both personnel and patients is minimized. This allows the equipment to operate safely without the need for external shielding, which not only reduces costs but also simplifies space design and enhances operational efficiency.

References.

1 Nadrljanski M., Walizai T., Campos A., *et al*. Computed tomography. Reference article, Radiopaedia.org (Accessed on 2 Dec 2024). DOI: /10.53347/rID-9027

2 Smith H., Hacking C., Chieng R., *et al*. Single photon emission computed tomography (SPECT). Reference article, Radiopaedia.org (Accessed on 2 Dec 2024). DOI: 10.53347/rID-62599

3 Hutton B. F. (2014). The origins of SPECT and SPECT-CT. European journal of nuclear medicine and molecular imaging, 41, 3-16. DOI: 10.1007/s00259-013-2606-5

4 Buck A. K., Nekolla S., Ziegler S., *et al*. (2008). SPECT-CT Journal of Nuclear Medicine, 49(8), 1305-1319. DOI: 10.2967/jnumed.107.050195

5 Gayed I. W., Kim, E. E., Broussard, W. F., *et al*. (2005). The value of 99mTc-sestamibi SPECT/CT over conventional SPECT in the evaluation of parathyroid adenomas or hyperplasia. Journal of Nuclear Medicine, 46(2), 248-252. PMID: 15695783

6 He B., Du Y., Song X., *et al*. (2005). A Monte Carlo and physical phantom evaluation of quantitative In-111 SPECT. Physics in Medicine & Biology, 50(17), 4169. DOI: 10.1088/0031-9155/50/17/018

7 Ketelhut S., Büermann L., and Hilgers, G. (2021). Catalog of x-ray spectra of Mo-, Rh-, and W-anode-based x-ray tubes from 10 to 50 kV. Physics in Medicine & Biology, 66(11), 115013. DOI: 10.1088/1361-6560/abfbb2

8 Valentin, J. (2007). The 2007 recommendations of the international commission on radiological protection (Vol. 37, No. 2-4, pp. 1-133). Oxford: Elsevier. DOI: 10.1016/j.icrp.2007.10.003

9 Podgorsak E. B. and Podgoršak E. B. (2014). Interaction of Photons with Matter. Compendium to Radiation Physics for Medical Physicists: 300 Problems and Solutions, 387-514. DOI: 10.1007/978-3-319-25382-4

10 Pelowitz D. B. (2005). MCNPX user's manual version 2.5. 0. Los Alamos National Laboratory, 76, 473.

11 Pelowitz D. B., Durkee J. W., Elson J. S.*et al*. (2011). MCNPX 2.7. 0 Extensions. Los Alamos National Laboratory, Los Alamos, NM, LA-UR-11-02295, 4.

Acknowledgments.

I would like to express my sincerest gratitude to all the people who made this project possible. To the INTEREST group for giving me the opportunity to improve myself and develop my skills in the field of physics. I especially want to thank my supervisor, Dr. Antonio Leiva Fabelo, for his help, presence, and unconditional patience. I would also like to thank my colleagues, Lic. Elizabeth Vega Moreno and Lic. Deniel Rodriguez Almora, for their support throughout this project. To all of them, thank you very much!